



Original research article

# Polarization splitter based on dual-core photonic crystal fiber with tellurite glass<sup>☆</sup>

He Feng-tao, Shi Wen-juan<sup>\*</sup>, Zhang Jian-lei, Hui Zhan-qiang, Zhan Fei

College of Electronic Engineering, Xi'an University of Posts and Telecommunications, Xi'an 710121, China

## ARTICLE INFO

### Article history:

Received 1 January 2018

Received in revised form 3 March 2018

Accepted 19 March 2018

### Keywords:

Photonic crystal fiber (PCF)

Polarization splitter

The full vector finite element method

Coupling length

Extinction ratio

## ABSTRACT

A polarization splitter based on dual-core photonic crystal fiber (PCF) with tellurite glass was proposed. The birefringence of the splitter was improved by introducing elliptical air holes. The full vector finite element method is used to analyze the impacts of structural parameters on the coupling length. The results show that the elliptical size is reasonably changed, the extinction ratio can reach 107.21 dB at the wavelength of 1.55  $\mu\text{m}$ , the length of the splitter is 89.05  $\mu\text{m}$ , and the bandwidth is 150 nm when the extinction ratio is more than 20 dB. Besides, we also compare the characteristics of tellurite glass and silica glass photonic crystal fiber polarization beam splitters with the same structural parameters.

© 2018 Published by Elsevier GmbH.

## 1. Introduction

High-speed, high-capacity all-optical network has become the trend of future communications. All-optical network with large capacity and ultra-high speed needs the support of high-performance optical devices, and all-optical devices with excellent performance and low price have become the research hotspots. Polarization splitter is an important optical device in all-optical network, which can separate one light beam into two orthogonal polarization states, the long length of a polarizing splitter made by a conventional optical fiber limits its application, so it is necessary to design a high-performance polarizing splitter.

Photonic crystal fiber (PCF), because of its unique and excellent optical properties, which include endlessly single-mode [1], ultra-low loss [2], high-birefringence [3], extremely effective mold field area [4], chromatic dispersion [5] and great nonlinearity [6] has attracted a large amount of interests since 1996. The flexible design of the structure and high birefringence provide the basis for high performance polarization splitter. So polarization splitter based on photonic crystal fiber has attracted research interest. At present, polarization splitters based on PCF have been reported. Rosa et al. [7] presented a polarization splitter consisting of square-lattice PCF, with the length being 29 mm, and the bandwidth being 90 nm when the extinction ratio is more than 23 dB. Rajeswari [8] designed a polarization splitter with dual-core PCF, with the length being 2 mm, and the bandwidth of the x, y-polarization modes being 100 nm and 55 nm. Saitoh et al. [9] proposed a three-core polarization splitter based on PCF, with the length being 1.9 mm, and the bandwidth being 37 nm. Jiang et al. [10] presented a dual-core polarization splitter based on PCF, whose length is only 119.1  $\mu\text{m}$ .

<sup>☆</sup> Foundation item: The National Natural Science Foundation of China (No. 61201193) and The Graduate Innovation Foundation of Xi'an University of Posts and Telecommunications (No. CXJJ2017009).

<sup>\*</sup> Corresponding author.

E-mail addresses: [hefengtao@xupt.edu.cn](mailto:hefengtao@xupt.edu.cn) (F.-t. He), [1143139693@qq.com](mailto:1143139693@qq.com) (W.-j. Shi).

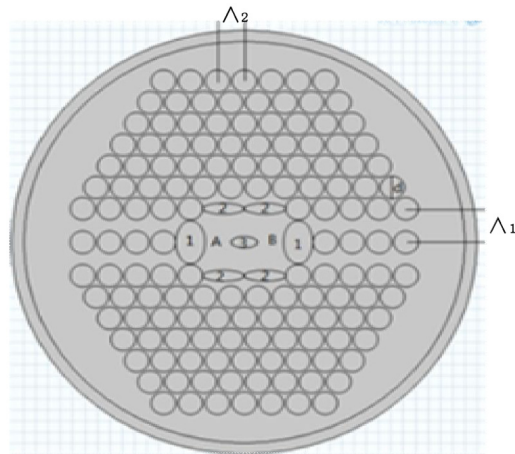


Fig. 1. Cross section of the polarization splitter.

Because the tellurite glass has a high linear and nonlinear refractive index and a wide transmission spectrum, especially, their typical melting temperature is much lower than that of silica, it has attracted researchers interests again. Liu [11] analyzed high extinction ratio PCF polarization splitter based on ZnTe glass, with the length being 1.1452 mm at the wavelength of 1.55  $\mu\text{m}$ , the extinction ratios being 92.16 dB and 29.56 dB in A and B cores respectively, and the bandwidth of the x, y-polarization modes being 100 nm and 45 nm. Liu et al. [12] analyzed a total solid three-core PCF polarization splitter based on tellurite, with the length being 1.14 mm, the extinction ratio being up to  $-101.27$  dB, the bandwidth being 100 nm. Liu [13] simulated a short and broadband polarization splitter based on PCF filled tellurite glass, with the length being 510  $\mu\text{m}$  at the wavelength of 1.55  $\mu\text{m}$ , the extinction ratio being 71.2 dB. Rui [14] proposed highly birefringent PCF polarization splitter made of soft glass, with the length being 252  $\mu\text{m}$  at the wavelength of 1.55  $\mu\text{m}$ , the extinction ratio being  $-44.42$  dB, the bandwidth being 32 nm. The above designs have their advantages, but they do not have the characteristics of short length, high extinction ratio and wide bandwidth, so the performance of polarization splitter should be further optimized.

In this paper, we proposed a polarization splitter based on dual-core photonic crystal fiber (PCF) with tellurite glass. The effective refractive index is calculated by the commercial package Comsol Multiphysics based on the full vector finite element method (FEM) with perfectly matched layer. Moreover, we analyzed the impacts of structural parameters on the coupling length, and by optimizing the structural parameters, a polarization splitter with ultra-short length, high extinction ratio and wide bandwidth is obtained. Besides, we also compared the characteristics of tellurite glass and silica glass photonic crystal fiber polarization beam splitters with the same structural parameters.

## 2. Model and theory

The cross section of the polarization splitter based on dual-core PCF with tellurite glass is shown in Fig. 1. The middle three rows of air holes are arranged in a rectangular lattice, the horizontal pitch is  $\Lambda_2 = 1.1 \mu\text{m}$  and vertical pitch is  $\Lambda_1 = 1.5 \mu\text{m}$ , the remaining circular air holes are arranged in a common hexagonal lattice and the diameter of circular air holes is  $d = 1.0 \mu\text{m}$  and a lattice constant is  $\Lambda_2$ . The minor and major half-axis length of the ellipse 1 are  $b_1 = 0.60 \mu\text{m}$  and  $a_1 = 0.97 \mu\text{m}$ , respectively. The distance between the ellipse 1 and the ellipse 3 in the horizontal pitch is  $2 \Lambda_1$ . The minor and major half-axis length of the ellipse 2 are  $b_2 = 0.25 \mu\text{m}$  and  $a_2 = 0.85 \mu\text{m}$ , respectively. The distance between the ellipse 2 and the ellipse 3 in the vertical pitch is  $\Lambda_1$ , and the horizontal direction between the two ellipses 2 is tangent. The minor and major half-axis length of the ellipse 3 are  $b_3 = 0.25 \mu\text{m}$  and  $a_3 = 0.53 \mu\text{m}$ , respectively. The background material of the whole fiber is ZnTe tellurite glass, the refractive index can be calculated from the Sellmeier formula [15], the material dispersion is negligible. The refractive index of the air is 1.

$$n(\lambda) = \sqrt{A + \frac{B\lambda^2}{\lambda^2 - C} + \frac{D\lambda^2}{\lambda^2 - E}} \quad (1)$$

where  $A = 2.4843245$ ,  $B = 1.6174321$ ,  $C = 0.053715551$ ,  $D = 2.4765135$ ,  $E = 225.0$ .  $\lambda$  is the free-space wavelength of the incident light and its unit is micrometer [15].

According to the mode coupling theory, there are four modes in the dual-core PCF, which are the odd-mode  $E_{xo}$ ,  $E_{yo}$  and even-mode  $E_{xe}$ ,  $E_{ye}$  in x, y-polarization directions, respectively [16]. Their field distributions of even modes and odd modes are shown in Fig. 2.

The same polarization mode that satisfying the interference conditions will cause the core power coupling, that is, the core power coupling is caused by the even and odd modes interference in the x, y-polarization directions [17]. When the energy of a polarized light is completely transferred from one core to another, that is, the optical power of the polarized

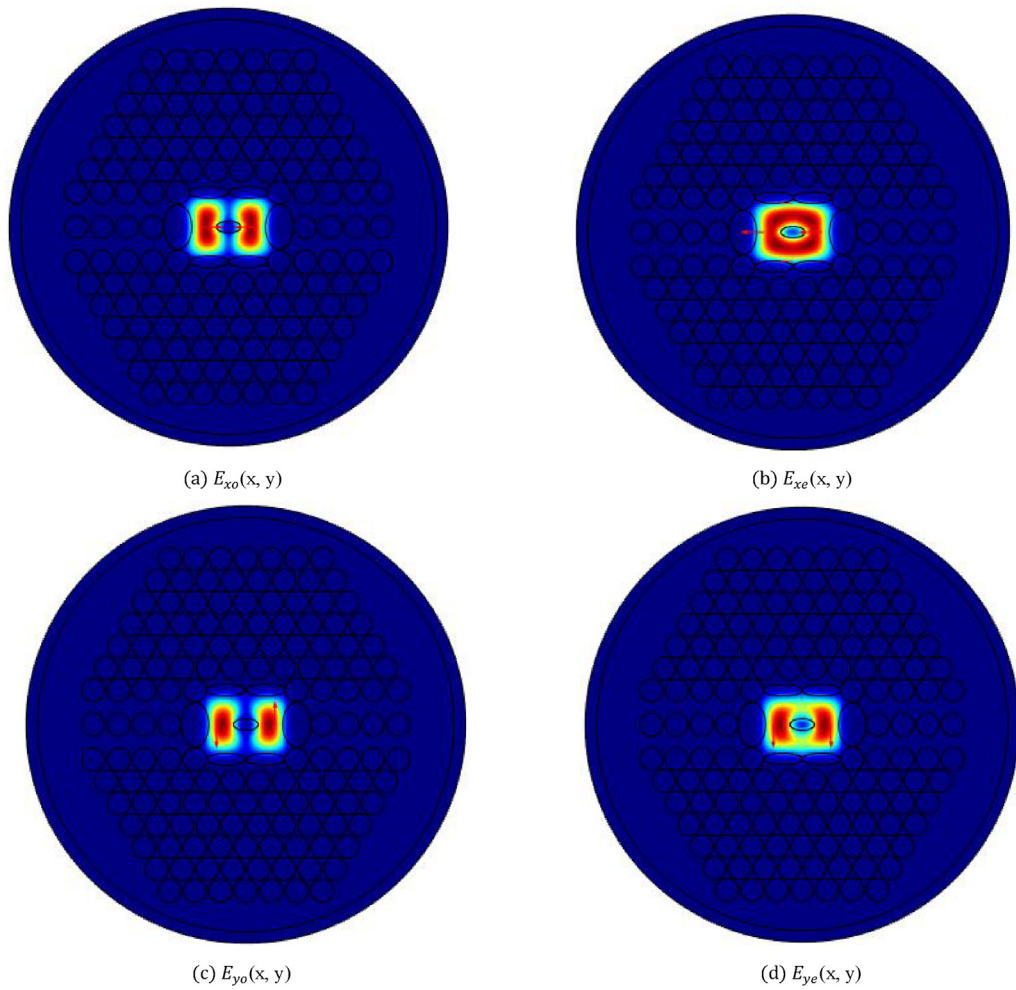


**Fig. 2.** Transverse magnetic-field vector distribution of the PCF.

light is changed from the maximum to the minimum, and the other core is changed from the minimum to the maximum, the distance traveled by the polarized light in the optical fiber is defined as the coupling length of the optical fiber [18].

$$L_{x,y} = \frac{\pi}{\beta_e^{x,y} - \beta_o^{x,y}} = \frac{\lambda}{2(n_e^{x,y} - n_o^{x,y})} \quad (2)$$

where  $\lambda$  is the wavelength of the incident light,  $\beta_e^x$  and  $\beta_o^x$ ,  $\beta_e^y$  and  $\beta_o^y$  are the propagation constants of x, y-polarized even and odd modes,  $n_e^x$  and  $n_o^x$ ,  $n_e^y$  and  $n_o^y$  are the effective refractive index of x, y-polarized even and odd modes, respectively.

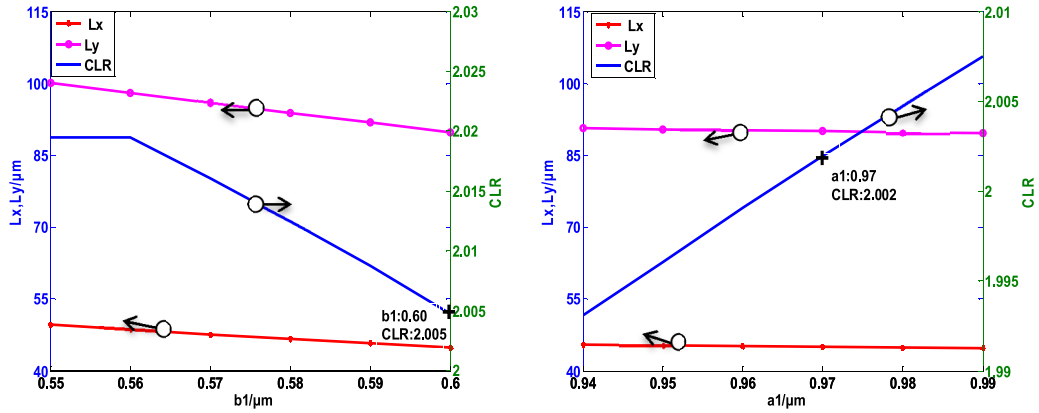
The length of splitter is an important parameter of the polarization splitter. Because the length of the polarization splitter is very short, its transmission loss can be neglected. When the input power of core A is  $p_{in}$ , the output powers of x, y-polarized light in core A are calculated from the following equation [7]:

$$P_{out}^{x,y} = P_{in} \cos^2 \left( \frac{\pi L}{2 L_{x,y}} \right) \quad (3)$$

$L_{x,y}$  can be calculated from Eq. (2).  $L$  is the length of fiber. Besides, the expression of normalized optical powers (NP) is:

$$NP_i = \frac{P_{out}^{x,y}}{P_{in}} = \cos^2 \left( \frac{\pi L}{2 L_{x,y}} \right) \quad (4)$$

When the length  $L$  of the fiber reaches  $L_s$ , the normalized optical power of a polarized light in the core region reaches a maximum value while the other reaches a minimum value,  $L_s$  is called the length of polarization splitter.



(a) Effect of  $b_1$ , the other parameters used are:

$$a_1=0.98, a_2=0.84, b_2=0.24, a_3=0.53, b_3=0.26$$

(b) Effect of  $a_1$ , the other parameters used are:

$$b_1=0.60, a_2=0.84, b_2=0.24, a_3=0.53, b_3=0.26$$

**Fig. 3.** The effect of the optimization of parameters  $b_1$  and  $a_1$  on the coupling length and the coupling ratio.

The extinction ratio (ER) is another important parameter to measure the performance of the polarization splitter. It is defined as the power of a particular polarization mode in the expected output core comparing to the power of the other polarization mode in the same core, which can be obtained as follows [19].

$$ER = 10 \log_{10} \frac{P_{out}^y}{P_{out}^x} \tag{5}$$

$P_{out}^x, P_{out}^y$  are the optical powers of the x, y-polarized light output port. The greater the absolute value of ER, the better the performance of polarization splitter. The two orthogonal polarization states of the incident light are regarded to be separated when the extinction ratio is greater than 20 dB [10], so ER determines the available bandwidth of a polarization splitter.

### 3. Results and discussions

Because of the coupling mode equations and the asymmetry for x, y-polarized direction, the coupling length is different in the PCF transmission, that is  $L_x \neq L_y$ , the dual-core PCF can be made into a polarization splitter. Coupling Length Ratio (CLR) is an important reference for designing a polarization splitter. It can be expressed as [20].

$$CLR = \frac{L_y}{L_x} = \frac{m}{n} \tag{6}$$

where  $m$  and  $n$  are integers with positive parity. To obtain a high-performance polarization splitter the CLR value is very close to 2 ( $L_x < L_y$ ) or  $1/2$  ( $L_x > L_y$ ). The key issue is how to adjust and optimize the structural parameters so that the value of CLR is very close to 2. Therefore, in order to achieve high-performance polarization splitter, there are six geometrical parameters to be adjusted and optimized, which are the major and minor half-axis of the ellipse 1, 2 and 3  $a_1, b_1, a_2, b_2, a_3, b_3$ , respectively.

The relation between the CL and CLR and the structural parameters of  $b_1, a_1$  are depicted in Fig. 3. Fig. 3(a) and (b) shows that  $L_x, L_y$  decrease as  $b_1$  and  $a_1$  increase. The main reason is when  $b_1, a_1$  increase, the birefringence is increased and the core mode field is reduced, the increase of birefringence is greater than the reduction of the core mode field, so  $L_x, L_y$  decrease with the increase of  $b_1, a_1$ . Besides, Fig. 3(a) shows that CLR first keeps level and then decreases as  $b_1$  increases, the main reason is that the increase in  $b_1$ , at the beginning, makes  $L_x, L_y$  descend at the same rate and then  $L_y$  descends faster than  $L_x$ , so CLR first keeps level and then decreases as  $b_1$  increases; While Fig. 3(b) shows that CLR increases as  $a_1$  increases, the main reason is that the increase in  $a_1$  makes  $L_y$  descends slower than  $L_x$ , so CLR increases as  $a_1$  increases. When the CLR value is very close to 2, we can obtain a high-performance polarization splitter, so we choose  $b_1 = 0.60 \mu\text{m}, a_1 = 0.97 \mu\text{m}$ . The relation between the CL and CLR and the structural parameters of  $b_2$  and  $a_2$  are depicted in Fig. 4. Fig. 4(a) and (b) shows that  $L_x, L_y$  increase as  $b_2$  and  $a_2$  increases. The main reason is when  $b_2, a_2$  increases, the birefringence is increased and the core mode field is more distributed in the cladding. This part of the energy weakens the core of the birefringence, so the coupling strength is weakened,  $L_x, L_y$  increase with the increase of  $b_2, a_2$ . Besides, Fig. 4(a) and (b) show that CLR increases as  $b_2$  and  $a_2$  increase, the main reason is that the increases in  $b_2, a_2$  makes  $L_y$  descends slower than  $L_x$ , so CLR increases as  $b_2, a_2$  increases. When the CLR value is very close to 2, we can obtain a high-performance polarization splitter, so we choose  $b_2 = 0.25 \mu\text{m}, a_2 = 0.85 \mu\text{m}$ . The relation between the CL, the CLR and the structural parameters of  $b_3$  and  $a_3$  are depicted in Fig. 5. Fig. 5(a) shows that  $L_x, L_y$  increase as  $b_3$  increases. The main reason is that when  $b_3$  increases, the birefringence is increased and the core mode field

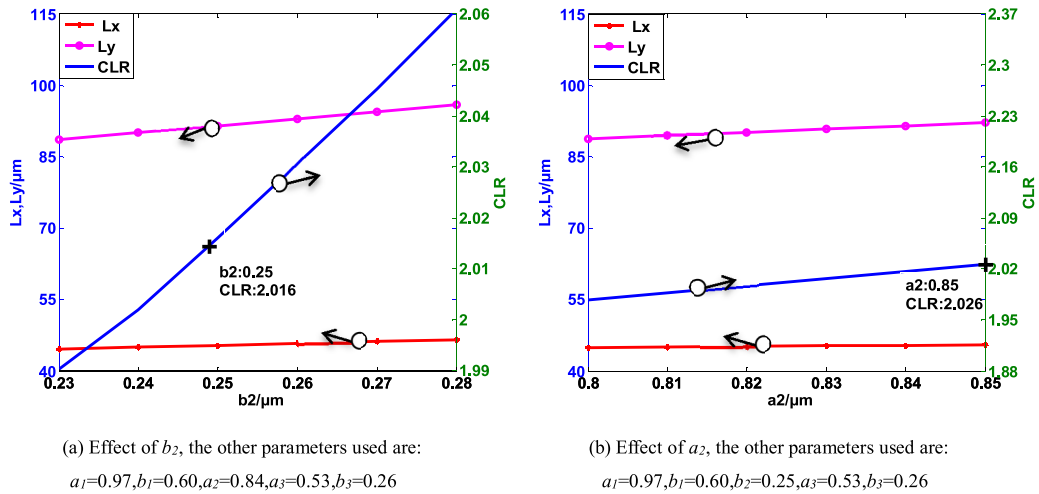


Fig. 4. The effect of the optimization of parameters  $b_2$  and  $a_2$  on the coupling length and the coupling ratio.

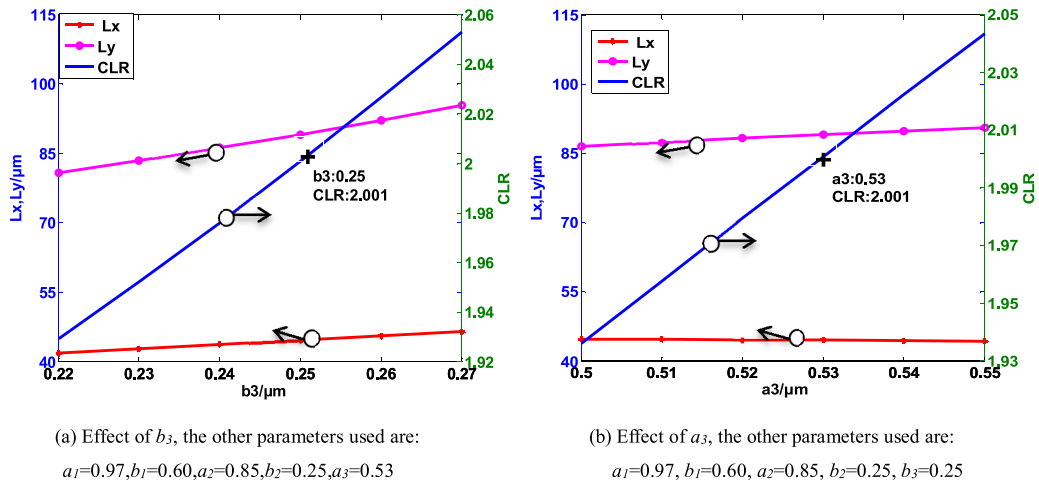


Fig. 5. The effect of the optimization of parameters  $b_3$  and  $a_3$  on the coupling length and the coupling ratio.

is reduced, and the core energy is continuously squeezed into the cladding, that is, the core mode field is more distributed in the cladding. This part of the energy weakened the core of the birefringence, so the coupling strength is weakened,  $L_x$ ,  $L_y$  increase with the increase of  $b_3$ . Fig. 5(b) shows that  $L_y$  increases as  $a_3$  increases, while  $L_x$  decreases as  $a_3$  increases, the main reason is that when  $a_3$  increases, the birefringence is increased and the core mode field is reduced, the increase of birefringence is greater than the reduction of the core mode field in the x direction but is opposite in the y direction, so  $L_y$  increases with the increase of  $a_3$ , while  $L_x$  decreases with the increase of  $a_3$ . Besides, Fig. 5(a) and (b) show that CLR increases as  $b_3$  and  $a_3$  increase, the main reason is that the increase in  $b_2$ ,  $a_2$  makes  $L_y$  descends slower than  $L_x$ , so CLR increases as  $b_3$  and  $a_3$  increase. When the CLR value is very close to 2, we can obtain a high-performance polarization splitter, so we choose  $b_3 = 0.25 \mu\text{m}$ ,  $a_3 = 0.53 \mu\text{m}$ .

Based on the above discussions, by adjusting and optimizing the structural parameters, the value of CLR can be very close to 2 and the optimized parameters are  $\Lambda_1 = 1.5 \mu\text{m}$ ,  $\Lambda_2 = 1.1 \mu\text{m}$ ,  $d = 1.0 \mu\text{m}$ ,  $a_1 = 0.97 \mu\text{m}$ ,  $b_1 = 0.60 \mu\text{m}$ ,  $a_2 = 0.85 \mu\text{m}$ ,  $b_2 = 0.25 \mu\text{m}$ ,  $a_3 = 0.53 \mu\text{m}$ ,  $b_3 = 0.25 \mu\text{m}$ . Fig. 6 shows the relation between the coupling length of tellurite, silica glass and the wavelength. It can be seen from Fig. 6 that the coupling length decreases as the wavelength increases. Besides, we can also see that at the wavelength of  $1.55 \mu\text{m}$ , the coupling length of tellurite glass is  $L_x = 44.51 \mu\text{m}$ ,  $L_y = 89.05 \mu\text{m}$  and the coupling length of silica glass is  $L_x = 25.74 \mu\text{m}$ ,  $L_y = 39.94 \mu\text{m}$ .

Core A and core B are symmetrical, so we analyze the normalized optical power of fundamental modes in core A. Fig. 7 shows the normalized optical power of tellurite and silica glass with the variations of propagation distance. The two orthogonal polarized optical powers are different at different fiber lengths, which are periodically shifted in cores A and B for x, y polarization directions. From Fig. 7(a) we can see that in the PCF polarization splitter based on tellurite glass, when the fiber length is  $89.05 \mu\text{m}$ , x polarized light couple into core B while y polarized light still in core A, i.e., they are separated from each other at the length of  $89.05 \mu\text{m}$ . From Fig. 7(b) we can see that in the PCF polarization splitter based on silica

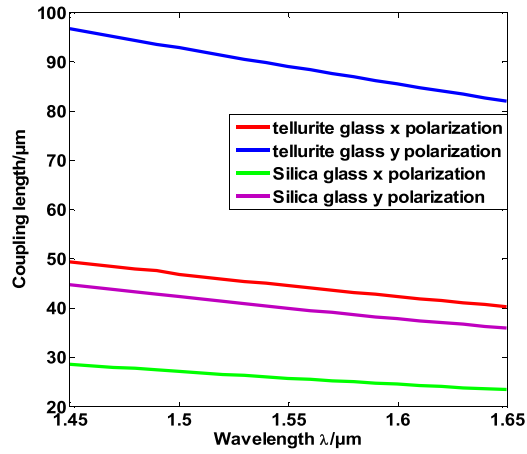


Fig. 6. Coupling length of X and Y polarization.

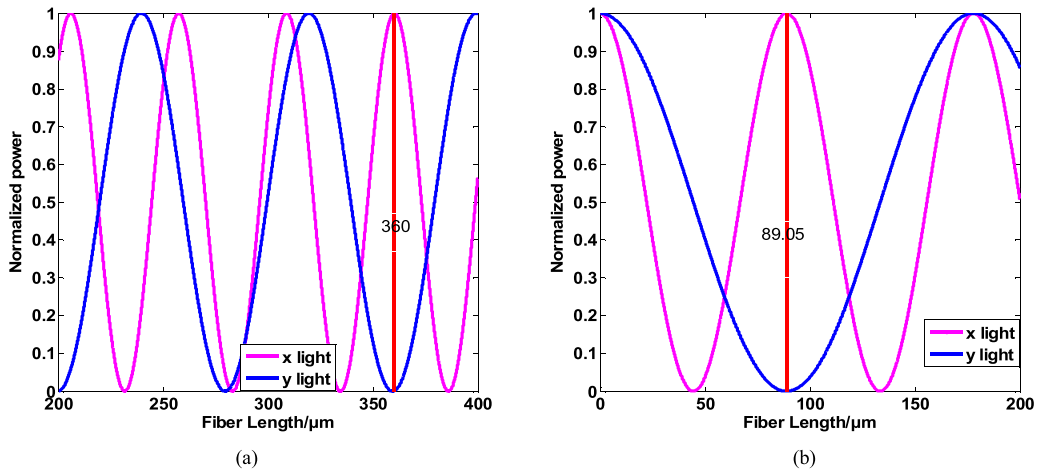


Fig. 7. Normalized power in core A versus fiber length (a) tellurite glass (b) Silica glass.

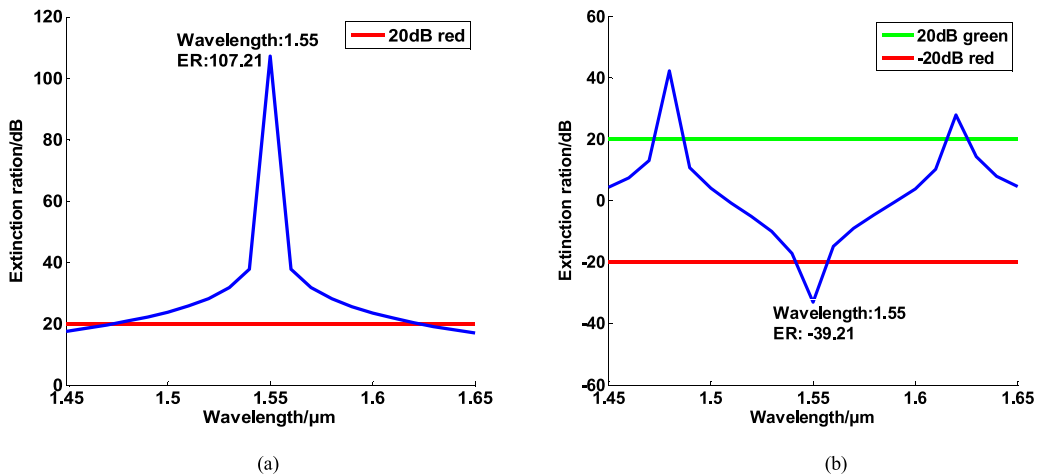


Fig. 8. Dependence of ER with wavelength in PCF polarization splitter (a) tellurite glass (b) Silica glass.

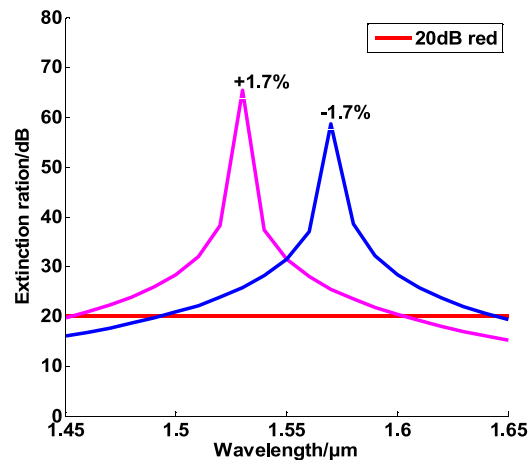


Fig. 9. ER varies with wavelength when the fiber error  $\pm 1.7\%$ .

glass, when the fiber length is  $360 \mu\text{m}$ , x polarized light couple into core B while y polarized light still in core A, i.e., they are separated from each other at the length of  $360 \mu\text{m}$ . What is more, the length of the PCF polarization splitter based on silica glass is longer than the PCF polarization splitter based on tellurite glass.

Fig. 8 shows the relation between ER and the wavelength. From Fig. 8(a) it can be seen that the largest value of ER of the polarization splitter based on tellurite glass is  $107.21 \text{ dB}$  at the wavelength of  $1.55 \mu\text{m}$ , and the bandwidth is  $150 \text{ nm}$  from  $1.473 \mu\text{m}$  to  $1.623 \mu\text{m}$ , covering the S, C and L bands when the ER is more than  $20 \text{ dB}$ . Fig. 8(b) shows that the ER of the polarization splitter based on silica glass is only  $32.91 \text{ dB}$  at the wavelength of  $1.55 \mu\text{m}$ , and the bandwidth is only  $25 \text{ nm}$  when the ER is more than  $20 \text{ dB}$ , and the bandwidth is  $16 \text{ nm}$  when the ER is less than  $-20 \text{ dB}$ . Therefore, the PCF polarization splitter based on tellurite glass has a better performance than the silica glass in the proposed dual-core PCF.

There will be fabrication tolerance in the practical production process, so the polarization splitter requires some fault tolerance. We analyze the influences of the slight changes of the splitter length on the extinction ratio and bandwidth. The results are shown in Fig. 9. From Fig. 9 we can see that the bandwidth almost does not change with the slight changes of the splitter length, when the error is  $\pm 1.7\%$ , and the bandwidth keeps  $150 \text{ nm}$ , the extinction ratio remains above  $20 \text{ dB}$  when the wavelength is  $1.55 \mu\text{m}$ , therefore, it has a high application value.

#### 4. Conclusions

To summarize, polarization splitter based on dual-core photonic crystal fiber (PCF) with tellurite glass was proposed. The full vector finite element method is used to analyze the impacts of structural parameters on the coupling length. Besides, we also compare the characteristics of tellurite glass and silica glass photonic crystal fiber polarization beam splitters with the same structural parameters and we find that the PCF polarization splitter based on tellurite glass has a shorter length, a higher ER and a wider bandwidth. The length of the splitter is  $89.05 \mu\text{m}$ , the bandwidth is  $150 \text{ nm}$  from  $1.473 \mu\text{m}$  to  $1.623 \mu\text{m}$  covering the S, C and L bands when the ER is more than  $20 \text{ dB}$ , and the ER can reach  $107.21 \text{ dB}$  at the wavelength of  $1.55 \mu\text{m}$ . At the same time, the polarization splitter has good fault tolerance characteristics. It still has a good performance when the error in the length of the polarization splitter is within  $\pm 1.7\%$ . It can be widely used in all-optical network.

#### Acknowledgments

This work was supported by the National Natural Science Foundation of China (Grant No. 61201193) and the Graduate Innovation Foundation of Xi'an University of Posts and Telecommunications (Grant No. CXJJ2017009)

#### References

- [1] H. Lee, M. Schmidt, H. Tyagi, L. Prill Sempere, P. Russell, Polarization-dependent coupling to plasmon modes on submicron gold wire in photonic crystal fiber, *Appl. Phys. Lett.* 93 (11) (2008) 111102.
- [2] B. Debord, M. Alharbi, A. Benoit, Ultra low-loss hypocycloid-core Kagome hollow-core photonic crystal fiber for green spectral-range applications, *Opt. Lett.* 39 (21) (2014) 6245–6248.
- [3] A. Ortigosa-Blanch, J.C. Knight, W.J. Wadsworth, et al., Highly birefringent photonic crystal fiber, *Opt. Lett.* 25 (18) (2000) 1325–1327.
- [4] J.C. Knight, T.A. Birks, R.F. Cregan, P.S.J. Russell, P.D. de Sandro, Large mode area photonic crystal fibre, *Electron. Lett.* 34 (13) (1998) 1347–1348.
- [5] M. Aliramezani, S.M. Nejad, Numerical analysis and optimization of a dual-concentric-core photonic crystal fiber for broadband dispersion compensation, *Opt. Laser Technol.* 42 (8) (2010) 1209–1217.
- [6] N. Broderick, T. Monro, P. Bennett, D. Richardson, Nonlinearity in holey optical fibers: measurement and future opportunities, *Opt. Lett.* 24 (22) (1999) 1395–1397.
- [7] L. Rose, F. Poli, M. Foroni, et al., Polarization splitter based on a square-lattice photonic crystal fiber, *Opt. Lett.* 31 (4) (2006) 441–443.

- [8] D. Rajeswari, A. Sivanantha Raja, S. Selvendran, Design and analysis of polarization splitter based on dual-core photonic crystal fiber, *Opt.-Int. J. Light Electron Opt.* 144 (2017) 15–21.
- [9] K. Saitoh, Y. Sato, M. Koshiba, Polarization splitter in three core photonic crystal fiber, *Opt. Express* 12 (17) (2004) 3940–3946.
- [10] Haiming Jiang, Erlei Wang, Jing Zhang, et al., Polarization splitter based on dual-core photonic crystal fiber, *Opt. Express* 22 (25) (2014) 30461–30466.
- [11] Qiang Liu, Shu-Guang Li, Zhenkai Fan, Wan Zhang, Jianchen Zi, Hui Li, Numerical analysis of high extinction ratio photonic crystal fiber polarization splitter based on ZnTe glass, *Opt. Fiber Technol.* 21 (2015) 193–197.
- [12] Zhaolun Liu, Haili Du, Ming Wang, All-solid three-core photonic crystal fiber polarization splitter, *Acta Photonica Sin.* 45 (10) (2016), 1023002-1-5.
- [13] Qiang Liu, Shuguang Li, Xinyu Gao, Xinxing Feng, Simulation of a short and broadband polarization splitter based on photonic crystal fiber filled with tellurite glass, *Opt. Quantum Electron.* 49 (60) (2017) 1–9.
- [14] Hao Rui, Highly birefringent photonic crystal fiber polarization splitter made of soft glass, *Opt.-Int. J. Light Electron Opt.* 125 (2014) 6757–6760.
- [15] L. Shuo, L. Shuguang, D. Ying, Analysis of the characteristics of the polarization splitter based on tellurite glass dual-core photonic crystal fiber, *Opt. Laser Technol.* 44 (6) (2012) 1813–1817.
- [16] N.J. Florous, K. Saitoh, M. Koshiba, Synthesis of polarization-independent splitters based on highly birefringent dual-core photonic crystal fiber platforms, *IEEE Photonics Technol. Lett.* 18 (11) (2006) 1231–1233.
- [17] Wang Zhi, Jian Shuisheng, Lou Shuqin, et al., Modal interference in dual-core photonic crystal fiber, *Acta Phys. Sin.* 53 (8) (2004) 2600–2606.
- [18] S.S. Zhang, W.G. Zhang, P.C. Geng, et al., Design of single-polarization wavelength splitter based on photonic crystal fiber, *Appl. Opt.* 50 (36) (2011) 6576–6582.
- [19] Lu Wengliang, Lou Shuqin, Wang Xing, et al., Ultrabroadband polarization splitter based on three-core photonic crystal fibers, *Appl. Opt.* 52 (3) (2013) 449–455.
- [20] Fu Bo, Li Shuguang, Yao Yanyan, et al., Coupling characteristics of high birefringence dual-core photonic crystal fiber, *Acta Phys. Sin.* 58 (11) (2009) 7708–7715.